HAL
open science

Quantified sensitivity of small lake sediments to record historic earthquakes: Implications for paleoseismology

Bruno Wilhelm, Jerome Nomade, Christian Crouzet, Camille Litty, Pierre Sabatier, Simon Belle, Yann Rolland, Marie Revel, Françoise Courboulex, Fabien Arnaud, et al.

To cite this version:

Bruno Wilhelm, Jerome Nomade, Christian Crouzet, Camille Litty, Pierre Sabatier, et al.. Quantified sensitivity of small lake sediments to record historic earthquakes: Implications for paleoseismology. Journal of Geophysical Research: Earth Surface, 2016, 121 (1), pp.2 - 16. 10.1002/2015JF003644 . hal-01880682

HAL Id: hal-01880682

https://sde.hal.science/hal-01880682v1

Submitted on 20 May 2021

HAL is a multi-disciplinary open access archive for the deposit and dissemination of scientific research documents, whether they are published or not. The documents may come from teaching and research institutions in France or abroad, or from public or private research centers.

L'archive ouverte pluridisciplinaire **HAL**, est destinée au dépôt et à la diffusion de documents scientifiques de niveau recherche, publiés ou non, émanant des établissements d'enseignement et de recherche français ou étrangers, des laboratoires publics ou privés.

AGU PUBLICATIONS

JGR

Journal of Geophysical Research: Earth Surface

RESEARCH ARTICLE

10.1002/2015JF003644

Key Points:
- Quantification of the sensitivities of eight lakes to record earthquakes
- The dominant control on the lake's sensitivity is sedimentation rate

Supporting Information:
- Texts S1 and S2, Figures S1–S5, and captions for Tables S1 and S2
- Table S1
- Table S2

Correspondence to:
B. Wilhelm,
bruno.wilhelm@ujf-grenoble.fr

Citation:
Wilhelm, B., et al. (2016), Quantified sensitivity of small lake sediments to record historic earthquakes: Implications for paleoseismology, *J. Geophys. Res. Earth Surf.*, *121*, 2–16, doi:10.1002/2015JF003644.

Received 15 JUN 2015
Accepted 26 NOV 2015
Accepted article online 7 DEC 2015
Published online 5 JAN 2016

©2015. American Geophysical Union. All Rights Reserved.

Quantified sensitivity of small lake sediments to record historic earthquakes: Implications for paleoseismology

Bruno Wilhelm[1,2,3], Jerome Nomade[4], Christian Crouzet[5], Camille Litty[1], Pierre Sabatier[6], Simon Belle[7], Yann Rolland[8], Marie Revel[8], Françoise Courboulex[8], Fabien Arnaud[6], and Flavio S. Anselmetti[1,2]

[1]Institute of Geological Sciences, University of Bern, Bern, Switzerland, [2]Oeschger Centre for Climate Change Research, University of Bern, Bern, Switzerland, [3]LTHE, University of Grenoble Alpes, Grenoble, France, [4]CNRS, ISTerre, University Grenoble Alpes, Grenoble, France, [5]CNRS, ISTerre, Université Savoie Mont Blanc, Le Bourget-du-Lac, France, [6]CNRS, EDYTEM, Université Savoie Mont Blanc, Le Bourget-du-Lac, France, [7]Chrono-environnement, Université Bourgogne Franche-Comté, Besançon, France, [8]CNRS, IRD, OCA, Géoazur, Université Nice Sophia Antipolis, Nice, France

Abstract Seismic hazard assessment is a critical but challenging issue for modern societies. A key parameter to be estimated is the recurrence interval of damaging earthquakes. This requires the establishment of earthquake records long enough to be relevant, i.e., far longer than historical observations. We study how lake sediments can be used for this purpose and explore conditions that enable lake sediments to record earthquakes. This was achieved (i) through the compilation of eight lake-sediment sequences from the European Alps to reconstruct chronicles of mass movement deposits and (ii) through the comparison of these chronicles with the well-documented earthquake history. This allowed 24 occurrences of mass movements to be identified, of which 21 were most probably triggered by an earthquake. However, the number of earthquake-induced deposits varies between lakes of a same region, suggesting variable thresholds of the lake sequences to record earthquake shaking. These thresholds have been quantified by linking the mass movement occurrences in a single lake to both intensity and distance of the triggering earthquakes. This method offers a quantitative approach to estimate locations and intensities of past earthquake epicenters. Finally, we explored which lake characteristics could explain the various sensitivities. Our results suggest that sedimentation rate should be larger than 0.5 mm yr^{-1} so that a given lake records earthquakes in moderately active seismotectonic regions. We also postulate that an increasing sedimentation rate may imply an increasing sensitivity to earthquake shaking. Hence, further paleoseismological studies should control carefully that no significant change in sedimentation rates occurs within a record, which could falsify the assessment of earthquake recurrence intervals.

1. Introduction

A well-dated and quantitative earthquake history is required for the assessment of long-term probabilistic seismic hazard [e.g., *Gürpinar*, 2005; *Mugnier et al.*, 2013]. However, the recurrence interval of strong earthquakes often exceeds the time span covered by instrumental and historical records in moderately active seismo-tectonic regions [e.g., *Michetti et al.*, 2005]. Hence, extending time series of seismic events is a key issue for understanding regional seismicity and for assessing the earthquake-hazard potential of such regions [e.g., *Becker et al.*, 2005; *Strasser et al.*, 2006; *Garrett et al.*, 2013; *Avşar et al.*, 2014].

Lake sediments provide suitable geological archives for reconstructing long-term earthquake occurrences. They are often continuous archives in which mass movement deposits and related turbidites triggered by historical earthquakes can be identified and dated in moderately [e.g., *Doig*, 1990; *Strasser et al.*, 2006; *Beck*, 2009; *Rodriguez-Pascua et al.*, 2010; *Strasser et al.*, 2013; *Petersen et al.*, 2014; *Brooks*, 2015] to highly seismogenic areas [e.g., *Ben-Menahem*, 1976; *Migowski et al.*, 2004; *Arnaud et al.*, 2006; *Boës et al.*, 2010; *Moernaut et al.*, 2014]. However, two main points still limit the achievement and use of such reconstructions; (i) the link between such deposits and their seismic trigger is not straightforward because other triggers are possible [e.g., *Monecke et al.*, 2004; *Van Daele et al.*, 2015], and (ii) epicentral locations and magnitudes of prehistoric earthquakes remain difficult to assess [e.g., *Michetti et al.*, 2005]. To date, three studies succeeded to estimate such parameters for past earthquakes by linking deposits in different lakes to seismic intensities in Switzerland [*Monecke et al.*, 2004; *Strasser et al.*, 2006] and, more recently, in Chile [*Moernaut et al.*, 2014] and New Zealand [*Howarth et al.*,

2014]. The approach developed in those studies highlights that each lake system has its own sensitivity to record earthquakes and that this lake sensitivity is critical in the estimation of epicentral locations and magnitudes of past earthquakes. However, it remains important to quantify lake sensitivity to seismic shaking in a range of setting and more importantly to determine what controls this sensitivity.

Previous studies of five small lakes in French Alps have highlighted the usefulness of their sediment sequences for assessing the regional earthquake hazard [*Arnaud et al*., 2002; *Nomade et al*., 2005; *Brisset et al*., 2012; *Wilhelm et al*., 2012, 2013]. Through the compilation of these five lake-sediment sequences with three new lakes in the same Alpine region, we aim at determining (i) the probability that the mass movement deposits were triggered by an earthquake and (ii) the potential links between earthquake magnitude, lake-epicenter distance, and lake-system parameters that both will improve the quality of lake sediment based paleoseismic investigations. This is undertaken through the comparison of our results with the historical seismicity, which is well documented over the last 500 years.

2. Regional Setting

2.1. Seismic Activity in the Western Alps

The Alps are one of the most seismically active regions of western Europe (Figure 1). The earthquakes focal mechanisms computed for the largest events ($M > 3.5$) that occurred since the development of good seismological networks (i.e., since ca. 1990) depict various present-day tectonic regimes. Some regions appears to be extensional [e.g., *Eva et al*., 1998; *Sue et al*., 1999; *Delacou et al*., 2004], while other areas are mainly affected by compression [e.g., *Thouvenot et al*., 1998; *Larroque et al*., 2009]. In addition, few main strike-slip faults with directions roughly N140°E and N30°E [e.g., *Tricart*, 1984] have been detected by different approaches [e.g., *Thouvenot et al*., 2003; *Courboulex et al*., 2007; *Cushing et al*., 2008; *Sanchez et al*., 2010; *Darnault et al*., 2012], which are and suspected to be active. However, whatever the tectonic regime in a given area, the ground motions generated are roughly the same [e.g., *Gregor et al*., 2014] so that the different types of stress nature were not considered in our study.

Most of the instrumental earthquakes recorded in the Alps by French, Italian, and Swiss networks are superficial (5 to 25 km depth) [*Eva et al*., 1998]. It is often difficult to unambiguously link their locations with well known faults, except for some particular cases. Instrumentally recorded magnitudes are usually smaller than Mw = 4 [*Cara et al*., 2015], although few events have a magnitude between 4 and 5. The most recent one that occurred in 2014 near Barcelonnette in the Southern Alps (Mw = 4.9) caused a lot of damage to infrastructure [*Marçot et al*., 2014] and generated macroseismic intensities of VI (French central seismological office) in the epicentral region.

Numerous evidence points to much larger events that occurred in the past. However, since they were not recorded by seismic networks, their magnitudes are assessed through evaluating macroseismic intensities. Historical earthquakes catalogs report that the Western Alps underwent earthquakes with macroseismic Medvedev-Sponheuer-Karnik (MSK) intensities up to IX and estimated magnitudes higher than 6., e.g., the Basel earthquake in 1356 (Mw = 6.6) [*Meghraoui et al*., 2000], the Visp earthquake in 1855 (Mw = 6.2) [*Fäh et al*., 2011], the Ligurian earthquake in 1887 (Mw = 6.8) [*Larroque et al*., 2012], and the Lambesc earthquake in 1909 (Mw = 6) [*Chardon and Bellier*, 2003]. These major earthquakes as well as smaller ones that caused damage are reported in the database SisFrance (http://www.sisfrance.net) [*Lambert and Levret-Albaret*, 1996; *Scotti et al*., 2004] (Figure 1), which is used in this study to keep the coherency between French, Italian, and Swiss events.

2.2. Studied Lake-Sediment Sequences in the Western Alps

The eight studied lakes are spread over three regions of the French Alps, for which the seismic activity is well established by historical records over the last 500 years (database SisFrance; Figure 1). Each sediment record can thus be compared with the respective local seismic activity. The studied lakes have small surface areas ($<1.1\ km^2$) and are characterized by various morphometries and lithologies (Table S1 in the supporting information). Sediment sequences of lakes Anterne (ANT), Blanc Aiguilles Rouges (BAR), Blanc Belledonne (BLB), and Foréant (FOR) are mainly composed of detrital material due to a high amount of easily erodible material in their catchment area, which is mobilized by frequent flood events [*Arnaud et al*., 2002; *Wilhelm et al*., 2012, 2013]. It generally results in a highly variable grain size and in high sedimentation rates

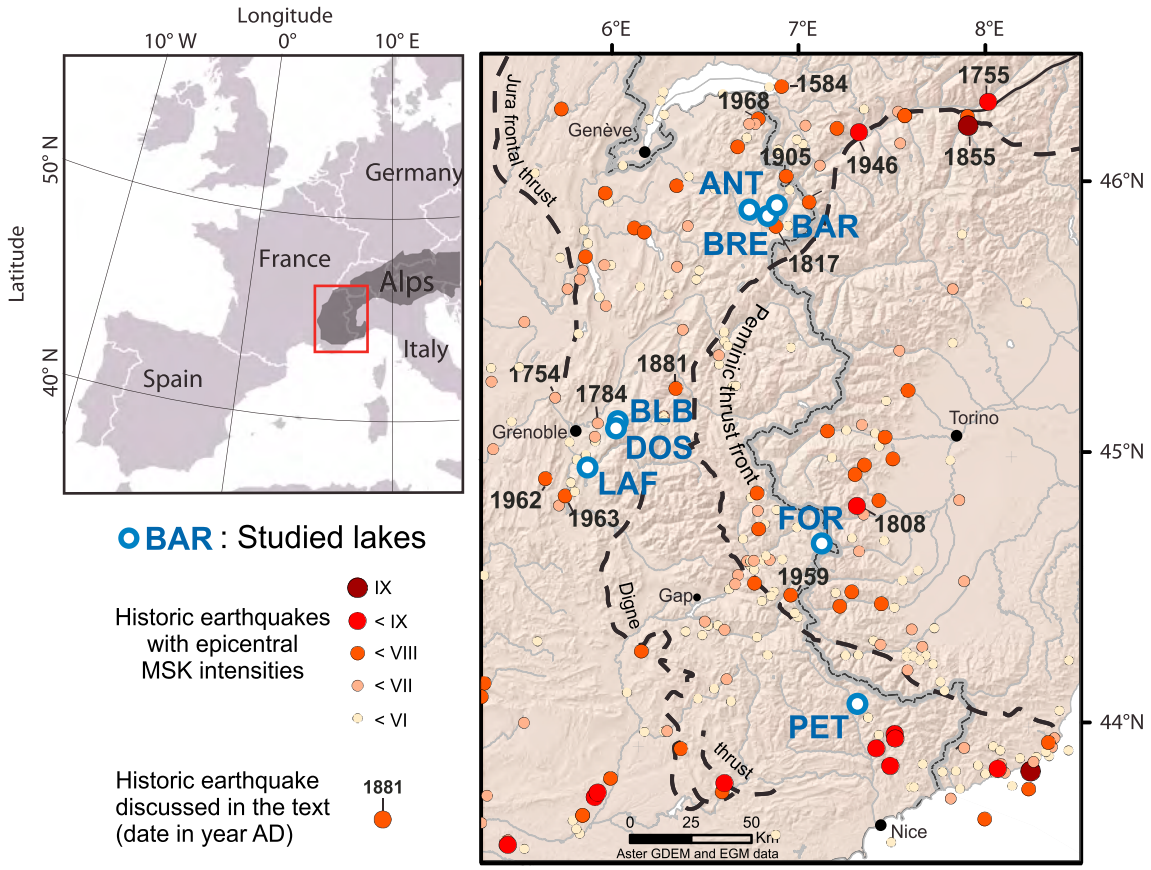

Figure 1. Location of the studied lakes in three regions of the French Alps and of all historic earthquakes with epicentral MSK intensity above IV. The earthquake catalog is provided by the database SisFrance (http://infoterre.brgm.fr/; BRGM, EDF, IRSN, and 2014). BAR: Lake Blanc Aiguilles Rouges [*Wilhelm et al.*, 2013], ANT: Lake Anterne [*Arnaud et al.*, 2002], BRE: Lake Brévent, BLB: Lake Blanc Belledonne [*Wilhelm et al.*, 2012], DOS: Lake Grand Doménon, LAF: Lake Laffrey [*Nomade et al.*, 2005], FOR: Lake Foréant, and PET: Lake Petit [*Brisset et al.*, 2012]. The dashed lines highlight the main overthrusts separating major Alpine tectonic units of the studied region.

($\geq$1 mm yr^{-1}). In contrast, sediments of lakes Brévent (BRE), Grand Doménon (DOS), and Petit (PET) are mainly composed of authigenic material (i.e., particulate organic matter and diatoms). As primary production is relatively low at their elevations, sedimentation rates are $\leq$0.7 mm yr^{-1} [e.g., *Brisset et al.*, 2012]. Lake Laffrey (LAF) is characterized by very high contents of detrital material, probably related to high soil erosion linked to human impact (agriculture/grazing), causing the highest sedimentation rate of 2.2 mm yr^{-1} [*Nomade et al.*, 2005]. The studied lakes are all situated directly on bedrock, except LAF which is emplaced on less than 15 m of glacial deposits [*Delaquaize*, 1979]. Hence, site effects resulting in local amplification of the ground motion may in these lakes be considered as negligible.

3. Methods

The common methods used in the previous studies to identify and date deposits associated to mass movement events, potentially related to palaeoearthquakes, are summarized here. For details and complementary methods, refer to the supporting information and to *Arnaud et al.* [2002] (Lake ANT), *Nomade et al.* [2005] (Lake LAF), *Brisset et al.* [2012] (Lake PET), *Wilhelm et al.* [2012] (Lake BLB), and *Wilhelm et al.* [2013] (Lake BAR).

To track mass movement deposits (MMDs) in the studied lake basins, a multicoring approach was first undertaken in almost all lakes because MMDs are often characterized by limited areal extent in the lake basins [e.g., *Moernaut et al.*, 2014]. The term "MMDs" includes here both the mass movement deposits (e.g., landslide deposits, slumps, and debris-flow deposits) and the related turbidites. Cores were then opened and photographed for a

detailed lithological description (color, lithology, sedimentary structures, deformed layers, etc.). In addition, grain size measurements were performed on retrieved cores to study the transport-deposition dynamics [e.g., *Passega*, 1964; *Shiki et al*., 2000; *Mulder et al*., 2001].

The chronologies of sequences ANT, BLB, LAF, and FOR are based on short-lived radionuclide (^{210}Pb, ^{137}Cs) measurements by gamma spectrometry and the application of the Constant Flux/Constant Sedimentation model allowing a mean sedimentation rate to be estimated over the last 150 years [*Goldberg*, 1963]. Ages of older MMDs for ANT, LAF, and BLB sequences were estimated by an extrapolated sedimentation rate over the last 250 years [*Arnaud et al*., 2002; *Wilhelm et al*., 2012] (Table 1). In the case of Lake BLB, the application of the ^{210}Pb dating method was not straightforward due to the high variability in sedimentation rate. Consequently, historical lead contaminations were investigated as additional chronostratigraphic markers with the peak of lead associated to the maximum use of leaded gasoline in 1973–1974 [*Renberg et al*., 2001; *Arnaud et al*., 2004]. Historical dates of local flood events were also considered as additional chronostratigraphic markers [*Wilhelm et al*., 2012].

Sequences BAR, PET, BRE, DOS, and FOR have been mainly dated by the ^{14}C method performed on macroremains of terrestrial plants to avoid a potential hard-water effect. The frequent occurrence of interbedded deposits in the BAR sequence and the low sedimentation rates of PET, BRE, and DOS sequences make the application of the short-lived radionuclide based chronology difficult [*Brisset et al*., 2012; *Wilhelm et al*., 2013] (supporting information). The calibration was undertaken using the Intcal09 calibration curve [*Reimer et al*., 2009] and the age-depth models were generated using the R-code package "clam" with a linear interpolation [*Blaauw*, 2010]. The resulting chronologies for Lakes BAR and FOR allowed regional flood signals to be reproduced at a decadal timescale [e.g., *Wilhelm et al*., 2013] (Figure S5). This supports the chronologies of these two sequences despite the large ^{14}C uncertainties.

The principal component analysis (PCA) performed in this study was achieved using the R software and FactoMineR package [*R Core Team*, 2012] on the main lake and sediment parameters.

4. Results

4.1. Mass Movement Deposits in Lakes ANT, BAR, BLB, LAF, and PET

Previous studies identified five types of MMDs (Figure 2 and Table 1) with their main characteristics briefly described here. For details, refer to the supporting information. Several studies provided a comprehensive overview of mass movement deposits [e.g., *Mulder and Cochonat*, 1996; *Mulder and Alexander*, 2001; *Gani*, 2004; *Mulder and Chapron*, 2011; *Strasser et al*., 2013; *Van Daele et al*., 2015], which are applied within this study. Two of the five MMDs types are sublacustrine landslide deposits, slumps, and debrites (Figure 2).

The two slumps identified in Lake BAR sequence are mainly characterized by a deformed structure and folded laminations [*Wilhelm et al*., 2013]. The lower boundaries of these deposits are marked by sharp contacts with the underlain undisturbed sediment. Within these deformed horizons, some laminations and event layers are still recognizable, and the grain size varies according to these sedimentary facies (Figure 2). Each of these deformed horizons has a limited extent; one has been recognized at the foot of the delta slopes and the other one at the foot of the opposite slope. Each deformed horizons is overlain by a graded turbidite that was also identified in most distal coring sites. Because of these characteristics, these deposits were interpreted as slumps, i.e., the deposition of mobilized sediment masses in slope-proximal areas. The graded turbidites overlying the slumps result from the sediment transported in suspension during the slope instability and eventually became deposited stratigraphically overlying the slump and reaching also further in the lake basin.

The six debrites in Lake LAF sequence are characterized by the lack of internal structure, a brown to blue color and a poorly sorted, medium to coarse silty sediment [*Nomade et al*., 2005]. The contacts to the underlying laminated sediment are sharp. These horizons are systematically overlain by a turbidite. In addition, cauliflower-shaped forms of carbonate concretions have been microscopically identified within the LAF horizons, suggesting a littoral sediment source. The lack of grading, the poor sorting, and the presence of littoral material suggest that these deposits are the result of debris flows coming from littoral sediment slopes (debrites). The overlying turbidites are interpreted as resulting from the particles that are transported in suspension during sliding, which eventually become deposited over a large area.

Table 1. List of All the MMDs Identified Over the Last 500 Years in the Eight Studied Lake Sequences[a]

Type of Mass Movement	Lake	Core	Core Depth (cm)	Criteria for a Mass Movement Origin for Graded Turbidites	Dating Methods	Dates of Deposits (AD)	Date of Historic Events (AD)	Differences Between Dates (year)	Differences Between Dates (%)	Reference
MS turbidite	ANT	ANT9902	14–15	-	210Pb + 137Cs	1966–1970 (1968)	1968	0	0	*Arnaud et al.* [2002]
MS turbidite	ANT	ANT9902	19–21	-	210Pb + 137Cs	1941–1948 (1945)	1946	1	1	
MS turbidite	ANT	ANT9902	29–34	-	210Pb + 137Cs	1900–1912 (1906)	1905	1	1	
MS turbidite	ANT	ANT9902	52.5–55.5	-	210Pb + 137Cs	1841–1859 (1851)	1855	4	3	
MS turbidite	ANT	ANT9902	63–66.5	-	Extrapolated Sed. Rate	1794–1817 (1807)	1817	10	5	
MS turbidite	ANT	ANT9902	68–69	-	Extrapolated Sed. Rate	1785–1809 (1797)	1785	12	6	
MS turbidite	ANT	ANT9902	77.5–78.5	-	Extrapolated Sed. Rate	1748–1776 (1762)	?	?	?	
MS turbidite	ANT	ANT9902	80–83	-	Extrapolated Sed. Rate	1735–1764 (1751)	1755	4	1.5	
Slump + Graded turb.	BAR	BAR09P1	6–36	1, 3	137Cs + 14C	1958–1998 (1991)	1986	5	20	*Wilhelm et al.* [2013]
Graded turbidite	BAR	BAR10II	23–28	3	14C	1866–1983 (1903)	1905	2	2	
Graded turbidite	BAR	BAR09P1	40–45	2	14C	1728–1968 (1813)	1817	4	2	
Slump + Graded turb.	BAR	BAR10II	55–61	1, 3	14C	1464–1804 (1595)	1584	9	2	
Debrite + Graded turb.	LAF	LAF0103	13–19	1	210Pb + 137Cs	1944–1970 (1957)	1963	6	12	*Nomade et al.* [2005]
Debrite + Graded turb.	LAF	LAF0103	19–24	1	210Pb + 137Cs	1944–1970 (1957)	1962	5	10	
Debrite + Graded turb.	LAF	LAF0103	33.5–40.5	1	210Pb	1889–1915 (1902)	1900–1910	0	0	
Debrite + MS turbidite	LAF	LAF0103	47.5–58	-	210Pb	1855–1881 (1868)	1881	13	10	
Debrite + MS turbidite	LAF	LAF0103	75–80	-	Extrapolated Sed. Rate	1774–1800 (1787)	1782	5	2	
Debrite + Graded turb.	LAF	LAF0103	88–94	1	Extrapolated Sed. Rate	1740–1766 (1753)	1754	1	0.5	
Graded turbidite	BLB	BLB0704	8.5–9	2	137Cs + Pb	1963–1970 (1966)	1963	3	7	*Wilhelm et al.* [2012]
Graded turbidite	BLB	BLB0704	9–9.5	2	137Cs + Pb	1963–1970 (1966)	1962	4	9	
MS turbidite	BLB	BLB0702	20.5–21.5	-	Extrapolated Sed. Rate	1879–1899 (1889)	1881	2	1.5	
Graded turbidite	BLB	BLB0704	39.5–40.5	2	Extrapolated Sed. Rate	1782–1825 (1803)	1782	20	9	
Debrite + Graded turb.	FOR	FOR13P4	7.5–8.5	1	210Pb + 137Cs	1959–1969 (1965)	1959	3	5	(unpublished data)
Debrite + Graded turb.	FOR	FOR13P4	27–44	1	14C	1775–1828 (1808)	1808	0	0	

[a]MS turbidite corresponds to Matrix-Supported turbidite. The criteria to determine the origin of the graded turbidites are (1) the spatial extent of the deposits, (2) their position on top of a slump or a debrite, and (3) a distinct pattern in a D90 versus deposit thickness diagram. See the text and supporting information for detailed explanations. The deposit ages between brackets correspond to the most probable age according to the age-depth model. Differences in year and percent between the deposit ages and the dates of probably associated historic event are also shown. References: ANT, *Arnaud et al.* [2002]; BAR, *Wilhelm et al.* [2013]; LAF, *Nomade et al.* [2005]; and BLB, *Wilhelm et al.* [2012].

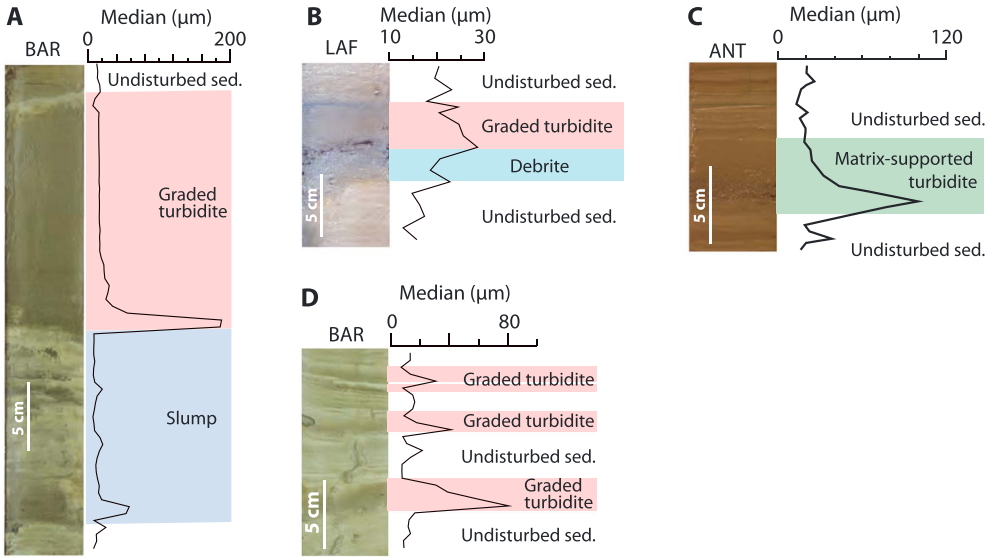

Figure 2. The five types of mass movement deposits identified through their macroscopic and grain-size features illustrated from sequences of Lakes BAR [*Wilhelm et al.*, 2013], ANT [*Arnaud et al.*, 2002], and LAF [*Nomade et al.*, 2005].

In addition, two types of turbidites related to these sublacustrine landslide deposits have been identified; matrix-supported, and graded turbidites (Figure 2).

The eleven matrix-supported turbidites, identified in lakes ANT and BLB, are characterized by poorly sorted fining-upward trends, i.e., matrix-supported turbidites [*Arnaud et al.*, 2002; *Wilhelm et al.*, 2012]. In Lake BLB, the matrix-supported turbidites have a spatial extent limited to the foot of a lateral slope, while they all reach the depocenter in Lake ANT. Their characteristic pattern in a Passega-type diagram (D50 versus D90) [*Passega*, 1964] is almost vertical, describing a large decrease of the coarse percentile (D90) without noticeable median (D50) variation [*Wilhelm et al.*, 2012]. These characteristics suggested that the transport energy is supplied by the sediment weight rather than by a water current velocity, i.e., formation of concentrated density flows of suspended sediments during a mass movement.

The numerous graded turbidites, identified in Lakes BAR, BLB, LAF, and FOR, are characterized by sharp boundaries to the underlying sediment, well-sorted fining-upward sequences and thin, whitish to bluish fine-grained capping layers [*Nomade et al.*, 2005; *Wilhelm et al.*, 2012, 2013]. The pattern of these graded layers in a Passega-type diagram is parallel to the D90 = D50 line [e.g., *Wilhelm et al.*, 2012, 2013]. These turbidites generally extend over a large area from the delta slope to the deep basin and its surrounding slopes. Only one of them in Lake BAR and two in Lake BLB have a spatial extent limited to the delta slope and the deep basin. In addition, one of these turbidites in Lake BAR and six in Lake LAF overlie a slump or a debrite. The good sorting suggests that the sediments were transported by turbidity flows. The fining-upward pattern mirrors a decreasing flow velocity and the thin whitish layer indicates the subsequent settling of the finest particles. Such layers were then interpreted as graded turbidites resulting from the deposits of turbidity flows. These turbidity flows can be induced by either flood events or mass movements [e.g., *Sturm and Matter*, 1978; *Mulder and Chapron*, 2011; *Wilhelm et al.*, 2015]. Based on three criteria (i) depositional geometry, (ii) position overlying a sublacustrine landslide deposit, and (iii) grain-size characteristics, 13 of all identified graded turbidites were interpreted as MMDs [*Nomade et al.*, 2005; *Wilhelm et al.*, 2012, 2013] (Table 1 and supporting information).

One can notice that no event layer was identified in Lake PET. Finally, the ages of each MMD are listed in Table 1.

4.2. Mass Movement Deposits in the New Lakes DOS, BRE, and FOR

The application of the established methods to the previously unstudied sequences reveals no event layer in Lake DOS and BRE sequences. In the Lake FOR sequence, numerous millimeter-to-centimeter-scale graded turbidites and three debrites overlain by graded turbidites occur (Table 1; see supporting information). The three graded turbidites on top of the debrites were associated to MMDs. For the other graded turbidites, there is no clear evidence to distinguish their origin between floods and MMDs.

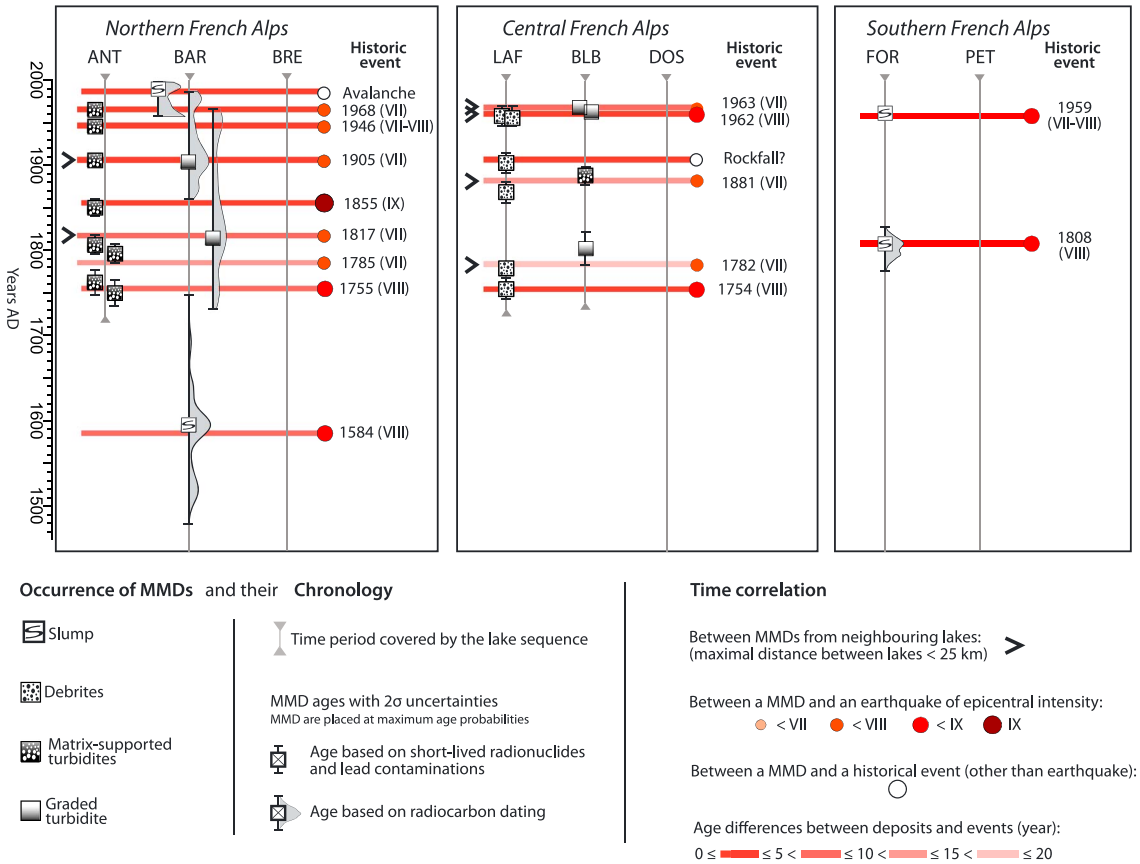

Figure 3. Temporal correlations between MMDs of neighboring lakes and between MMD occurrences and historical events over the last 500 years.

Mean sedimentation rates in lakes DOS and BRE were determined as 0.6 ± 0.08 and 0.3 ± 0.02 mm yr^{-1} over the last 500 years, respectively (see supporting information). Mean sedimentation rate in lake FOR was determined as 1 mm yr^{-1} over the last 500 years and the two youngest debrites dated within the last 500 years to A.D. 1959 ± 6 and A.D. 1808 ± 20 (Table 1).

Hence, 34 MMDs were identified and dated from the study of the eight lake sequences and correspond to 24 mass movement occurrences over the last 500 years (Table 1). This allowed us to reconstruct the mass movement chronicles for every lake (Figure 3).

5. Discussion

5.1. Determining the Trigger of the Identified Mass Movement Deposits

MMDs can be triggered by spontaneous failures due to overloading of slope sediments, snow avalanches, fluctuations in lake levels, rockfalls, or earthquakes [e.g., *Monecke et al.*, 2004; *Girardclos et al.*, 2007; *Van Daele et al.*, 2015]. Here changes of lake level can be excluded because water levels of all studied lakes are well controlled by bedrock outlets. An earthquake trigger can be identified by widespread mass movements, i.e., large scale or multiple, synchronous MMDs in a lake [e.g., *Schnellmann et al.*, 2006; *Fanetti et al.*, 2008; *Moernaut et al.*, 2007, 2014; *Beck*, 2009; *Strasser et al.*, 2013]. This approach, in our study expanded to multiple lakes, revealed that half (12 on 24) of the MMDs have synchronous events (within the 2σ-dating uncertainties) in neighboring lakes (ANT, BAR, and BLB, LAF, distance between lakes smaller than 25 km; Figure 3 and Table S1), supporting strongly an earthquake trigger for these MMDs. However, even high-magnitude earthquakes do not systematically trigger widespread MMDs [*Talling*, 2014, and references therein]. Therefore also when MMDs occur in only one lake, an earthquake trigger cannot be excluded. Hence, we use the temporal assignment of MMDs to their triggering earthquakes as a complementary way to determine the MMD trigger [e.g., *Beck*, 2009; *Boës et al.*, 2010; *Avşar et al.*, 2014; *Howarth et al.*, 2014; *Moernaut et al.*, 2014;

Talling, 2014]. MMD ages were then compared to (i) the dates of the regional historical earthquakes that generated epicentral MSK intensities larger than IV and that occurred closer than 150 km from the lake (database SisFrance) (Figure 1) and to (ii) the dates of other historical events known from documentary evidence, which affected some of the lake catchments [*Lignier*, 2001; *Nomade et al*., 2005]. This comparison highlights that 21 out of 24 of the identified MMDs are in agreement (within the noticeable 2σ-radiocarbon-dating uncertainties) with 15 historical earthquakes with epicentral intensity $\geq$VI and epicentral location closer than 100 km (Figure 3 and Table 1). The time correlation and the calculation of age differences were systematically conducted based on the most probable MMD ages, i.e., the highest age probabilities given by the age-depth model. These ages provided chronologies that allowed regional flood signals to be reproduced at a decadal timescale [e.g., *Wilhelm et al*., 2013] (Figure S5). Nevertheless, for Lake BAR sediments, unequivocal correlations between MMDs and specific earthquakes remain uncertain due to decadal-scale uncertainties of MMD ages and the relatively high number of potential triggering earthquakes.

The three uncorrelated MMDs are (i) the most recent slump at Lake BAR, (ii) a matrix-supported turbidites at Lake ANT, and (iii) a graded turbidite at Lake LAF. No coinciding major historical earthquake is recorded. However, an exceptionally large snow avalanche occurred in the BAR catchment in A.D. 1986, sweeping away the old mountain hut built close to the lake outlet, and covering the rocky lake outlet by sediments [*Lignier*, 2001, and references therein]. As such an event can trigger a mass movement [e.g., *Monecke et al*., 2004; *Vasskog et al*., 2011] and as the age of the slump is in agreement with the date of the avalanche, the avalanche was considered to be the cause of the MMD [*Wilhelm et al*., 2013] (Figure 3 and Table 1), and the event was not used in our paleoseismic database. In the LAF catchment, local witnesses reported the occurrence of a subaerial landslide around A.D. 1900–1910, possibly related to the artificial rise of the lake level [*Nomade et al*., 2005]. As such processes can trigger mass movements [e.g., *Monecke et al*., 2004; *Kremer et al*., 2012] and as the date is in the range of the turbidite age, the subaerial landslide was interpreted as the cause of the MMD [*Nomade et al*., 2005]. The origin of the uncorrelated matrix-supported turbidite in Lake ANT remains undetermined because no particular events are known at this time in its catchment [*Arnaud et al*., 2002]. Hence, 21 out of 24 of the MMDs were very probably triggered by historical earthquakes and 12 of which with very high likelihood.

5.2. Sensitivity of Lake Systems to Earthquake Shaking

5.2.1. Assessment of the Lake-System Sensitivity

The number of earthquake-triggered MMDs varies between lakes of a same region (Figure 3). For each region, we can observe a decrease of the MMD occurrence from ANT to BRE in the north, from LAF to DOS in the central part, and from FOR to PET in the south of the French Alps (Figure 3). This may suggest that the different lake sequences have a different sensitivity to slope instability caused by earthquake shaking. This variability in lake sensitivity was previously observed in Chilean lakes and termed Earthquake-Recording Threshold (EQRT) [*Moernaut et al*., 2014; *Van Daele et al*., 2015]. Those authors estimated the EQRT by linking the generation of a MMD to a minimum local seismic intensity. Here this approach cannot be applied because local seismic intensity, magnitudes, and/or shake maps are available for only very few earthquakes. To assess the respective sensitivity of each lake system to earthquake shaking, the epicentral intensities of all regional historic earthquakes were plotted against their distance from the lakes. Because the studied region is rather small and in the same kind of seismological context, it is reasonable to assume that ground motion attenuation be roughly the same in the entire zone. If we assume a uniform attenuation relationship for the entire area, historical earthquakes supposed to have triggered the MMDs are expected to be both the strongest and the closest to the lakes, as those are expected to have generated the largest ground motions in the lake areas. They should thus appear in the upper left corner of the 'epicentral intensity versus epicentral distance diagrams [*Ambraseys*, 1988; *Monecke et al*., 2004] (Figure 4a). Such diagrams highlight that the recorded earthquake-triggered MMDs correspond indeed to both the strongest and the closest events for each site (Figure 4b, red dots). An empirical limit was defined that separates recorded from nonrecorded earthquakes in each lake. This limit defines the sensitivity threshold specific to each lake. Thresholds were first defined for the sites of ANT, LAF, BLB, and FOR because their respective domains of recorded and nonrecorded earthquakes are well constrained (Figure 4b). The slopes of their sensitivity thresholds appear similar independent of the regional geology. This confirms the hypothesis that the attenuation of the seismic waves is approximately uniform

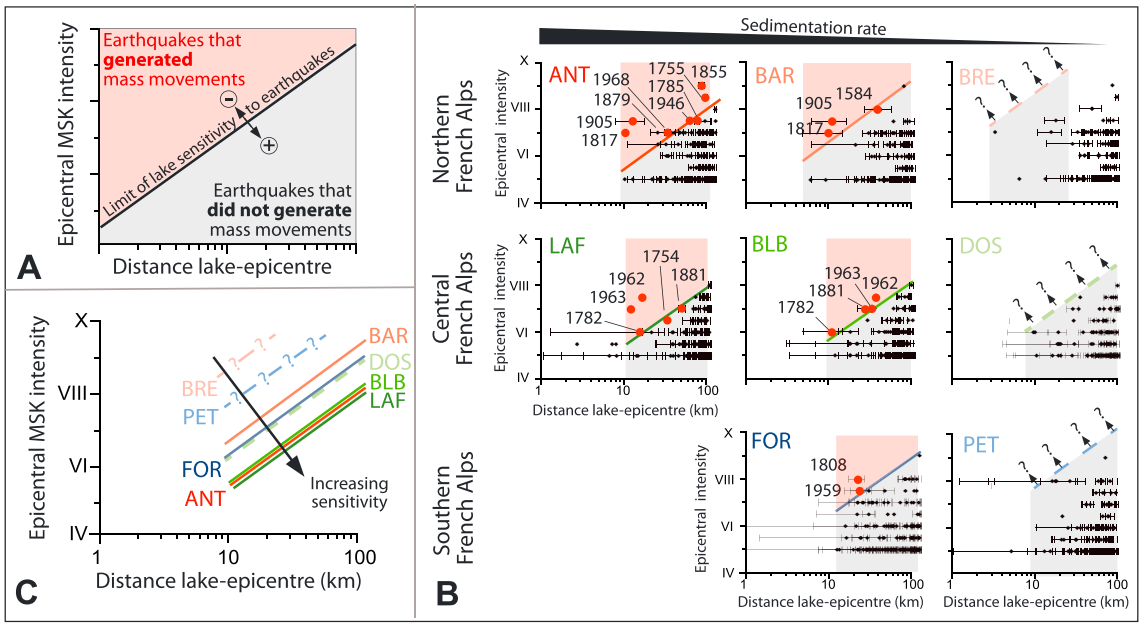

Figure 4. (a) Conceptual diagram "distance of earthquakes to the lake versus epicentral MSK intensity" for the assessment of the lake sensitivity to earthquakes. (b) Results from the eight studied lake sequences. Black crosses indicate all historic earthquakes closer than 100 km to the lakes with epicentral MSK intensities ≥IV with their respective location uncertainties (horizontal black bars). Red dots with dates correspond to historic earthquakes correlated to MMDs in Figure 7. For each lake, the limits of sensitivity (continuous lines) are placed to delimit the recorded from nonrecorded earthquakes. When no earthquake is recorded (DOS, BRE, and PET), the sensitivity limits (dotted lines) are placed at the maximum sensitivity possible. (c) Sensitivity limits of the eight lakes.

at the regional scale and that, in first order, the effects of the regional geology may be considered here as negligible. Thus, we kept the same slope ($a = 1.13$) for all diagrams in:

$$y = a.\ln(x) + b,$$

where x corresponds to the distance between the lake and the epicenter, y to the epicentral intensity of the historical earthquakes, a to the slope of the threshold line, and b to the intersection of the threshold line with the y axis. For BRE, DOS, and PET, the threshold lines were defined at the maximal possible sensitivity, as no events were recorded in the sediment of these lakes. All defined threshold lines were finally reported in a synthetic diagram (Figure 4c), which allows comparison between all lake sensitivities independently on their regional settings. One can notice that earthquakes of epicentral intensity V–VI occurring very close to Lake LAF (2.5–10 km) do not seem to have triggered any mass movement, while some mass movements identified at LAF and BLB were associated to earthquakes of epicentral intensity of VI (Figure 4b). For such short distances from the epicenter, local intensities are expected to be similar to epicentral intensities [*Bakun and Scotti*, 2006], suggesting that the threshold of minimum local seismic intensity to trigger a mass movement is slightly lower than VI. This threshold is very similar to those reported for some lakes in Chile [*Moernaut et al.*, 2014; *Van Daele et al.*, 2015] or New Zealand [*Howarth et al.*, 2014] but slightly lower than for some Swiss lakes (threshold of VI–VII) [*Monecke et al.*, 2004]. This reveals a relatively high sensitivity of some alpine-type lakes to earthquake shaking. In addition, one can notice that no earthquake occurring further than 100 km from lakes appears to be recorded. This can be related to the attenuation of the seismic waves with the distance. Indeed, based on the intensity attenuation equations of *Bakun and Scotti* [2006], an earthquake with a magnitude >6.5 should trigger local intensities ≥VI at 100 km distance from the epicenter. However, no historical earthquake with such a magnitude has been documented over the last 500 years in the Western Alps [database SisFrance, *Lambert and Levret-Albaret*, 1996; *Scotti et al.*, 2004; database ECOS09, *Fäh et al.*, 2011].

The synthetic diagram highlights that the lake sensitivities to earthquake shaking are highly variable (Figure 4c). An adapted EQRT [*Moernaut et al.*, 2014], called Earthquake-Sensitivity Threshold Index (ESTI), was then defined as the inverse of the intercept of the threshold lines with the intensity axis at 10 km from the lakes. The distance of 10 km was here used because of the scarcity of earthquakes at such short distances

that prevents the systematic assessment of the local seismic intensity threshold (Figure 4b). In addition, a ratio was adopted in order that the value of the ESTI increases with the lake sensitivity and vice versa. The highest sensitivity corresponds to ANT, BLB, and LAF with an ESTI above 0.18 indicating that mass movements can be triggered by nearby (~10 km) earthquakes reaching the minimal local intensity threshold (VI) or distant (<100 km) earthquakes of epicentral intensity of VIII. The sensitivity of FOR and BAR appears of "medium" order with an ESTI between 0.15 and 0.16. Mass movements can thus be triggered by nearby earthquakes of epicentral intensity VII or distant earthquakes of epicentral intensity of IX–X. The lowest sensitivity appears for BRE and PET as no mass movement was identified, despite the occurrence of intensity >VII earthquakes in their vicinity (Figure 4b). This suggests a maximal ESTI of 0.13 for these two lakes.

Moernaut et al. [2014] and *Van Daele et al*. [2015] have shown that the lake sensitivity of many lakes in the highly seismogenic area of Chile ranges from V¾ to VII½ . Our results suggest a similar range of lake sensitivity for lakes located in moderately seismogenic areas. This opens new perspectives in those areas for palaeoseismological reconstructions with the possibilities (i) to estimate the location of past epicenters by choosing several lakes of equal sensitivity spread in a region of ~100 km and (ii) to estimate epicentral intensities of past regional earthquakes by studying neighboring lakes of graded sensitivity. In addition, the ESTI method offers a new way to evaluate the lake sensitivity when information about the local seismic intensity is missing.

5.2.2. Possible Explanations for Distinct Lake Sensitivities

The varying lake sensitivities to earthquake shaking mirror varying susceptibilities of their slope toward failing. The stability of a sedimentary deposit on a given slope depends to a large extent on the slope angle, sediment thickness, and the geotechnical properties of the sedimentary succession potentially comprising weak layers [e.g., *Morgenstern*, 1967; *Strasser et al*., 2011; *Ai et al*., 2014; *Wiemer et al*., 2015]. Slope angle is a key parameter for a slope-stability assessment because it drives the destabilizing loading forces through gravity. Lower slope angles imply reduced loading forces and make slope sediments stable even in case of external forcing, i.e., earthquake shaking. Inversely, high slope angles imply high loading forces and may even result in spontaneous slope failures under static conditions. Above a certain threshold however, slopes become too steep to accumulate significant sediment for sliding. Generation of large slope-sediments failures related to earthquake shaking is thus usually limited to slope areas with intermediate angles steep enough to produce slides but not too steep for sediment accumulations. For the studied lakes, these values can be estimated from the positions of the localized MMDs and the angle of the nearest slopes. In Lake BAR, two slumps are restricted to the foot of slopes of around 20°. In Lake BLB, the two localized earthquake-triggered graded beds originate from slopes with angles ranging from 10 to 20°. In Lake FOR, the slope angle of the area surrounding the two slumps is also ~20°. Hence, slope angles ranging from 10 to 20° appear to be favorable for the generation of earthquake-triggered MMDs, which is in agreement with many studies [e.g., *Chapron et al*., 1999; *Schnellmann et al*., 2005; *Moernaut et al*., 2007; *Strasser et al*., 2007, 2011; *Bertrand et al*., 2008; *Van Daele et al*., 2013; *Doughty et al*., 2014]. We postulate that a larger spatial extent of intermediate-slope areas may favor a higher ESTI. To explore this link, the spatial extent of such areas was calculated for each lake basin using GIS (Geographic Information System) software (Table S1).

Sediment lithologies influence the slope stability by controlling the geotechnical ability to resist downslope forces. This ability can be assessed by measuring shear strength in situ or in sediment cores [e.g., *Chapron et al*., 1999; *Stegmann et al*., 2007; *Strasser et al*., 2011; *Ai et al*., 2014; *Wiemer et al*., 2015]. As these geotechnical data are not available, we analyzed the sedimentological properties responsible for shear strength variations to approach the origin of the ESTI variability, i.e., grain size, organic matter content, and the slope recharge capabilities that may be quantified through sedimentation rate (Table S1). Grain size appears particularly important for slope stability because it determines porosity-controlled properties (e.g., bulk density, water content, and void ratio) [*Baraza and Ercilla*, 1994] and notably acts on the shear strengths [e.g., *Ai et al*., 2014, and references therein]. For instance, undrained shear strength can be significantly reduced by small increases in sand content [*Lee et al*., 1987]. Moreover, the internal friction angle decreases when clay content increases, reflecting the low mobilized friction between fine particles [*Dhouib et al*., 2004]. In addition, coarse-grained material is generally characterized by a lower cohesion, which may imply reduced drained shear strength. However, higher grain size is also expected to increase permeability and, thereby, limits susceptibility toward pore-water overpressure that favors failures. Hence, both fine and coarse grain sizes can positively and negatively act on slope stability. To assess the role of the grain size on the ESTI, three parameters have thus been retained from the grain-size measurements: the clay (<2 μm) content, the coarser percentile

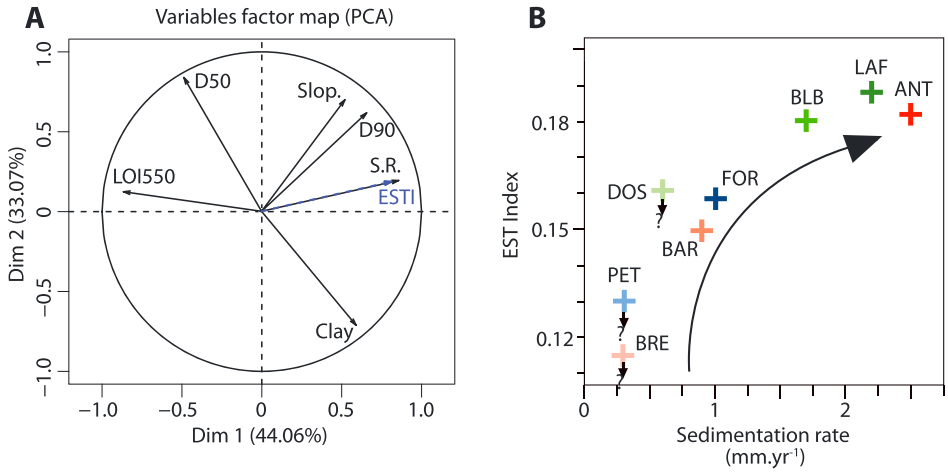

Figure 5. (a) Variable factor map resulting from the PCA on the lake's morphologic and sedimentologic parameters. Slope corresponds to the lake area of slopes between 10 and 20°. LOI550 corresponds to the organic matter content, S.R. to the basinal sedimentation rate, D50 to the median grain size, D90 to the coarser percentile, and Clay to the clay content. Earthquake-Sensitivity Threshold Index (ESTI) is added to this PCA as an illustrative variable (dashed blue line). (b) ESTI is plotted against the sedimentation rate. Arrows under DOS, BRE, and PET show that these ESTIs are maximum values.

(D90), and the median (D50). The median is used here as an integrative estimate of both parameters. Organic matter content (LOI550) generally implies lower bulk density and, thereby, lower loading forces on a given sedimentary deposits. However, the decomposition of organic matter can result in free gas in the sediments which can have a strong negative impact on slope stability. Finally, sedimentation rate (SR) may induce pore-fluid overpressure in low-permeability lithologies that favor slope instabilities but, in most cases, overpressure alone does not cause slope failure [*Ai et al.*, 2014, and references therein]. In addition, the sedimentation rate also influences the slope recharge potential required after a previous mass movement.

To explore the links between the ESTI and the lake's morphologic and sedimentologic parameters (10–20° slope area, organic matter content, clay content, D50, D90, and sedimentation rate), data from the eight lake systems were subjected to a PCA (Figure 5a). In an ideal case, data from the main slope sediments should be considered as they correspond to the sediment sources of the mass movements. As such data are not available, basinal sediments were here used to provide lake-specific proxies also for slope sediments. Due to the small size of the studied lakes, we assumed that a higher value of organic matter content (LOI550) or of sedimentation rate (SR) in the depocenter mirrors higher values on the slopes as well. Grain-size data (Clay, D50, and D90) from MMDs in the basin approximate slope-sediment characteristics, as these MMDs originate in the slope areas. When MMDs were absent in a lake sequence (i.e., Lake BRE, PET, and DOS), grain-size data corresponds to the "sedimentary background." The first principal component (Dim 1) explains 45.84% of the variance and shows high positive loadings for sedimentation rate and high negative loadings for organic matter content. Dim 2 explains 35.16% of the variance and gives positive loadings for D50 and D90 and at lesser extent for the 10–20° slope area and high negative loadings for clay content. The lake sensitivity, i.e., ESTI, is added to this PCA as an illustrative variable and thus did not enter the PCA calculation. This PCA clearly shows that the main controlling parameter on the ESTI is sedimentation rate with a significant correlation between these two parameters ($p = 0{,}003$; $r = 0.89$; Figure 5b). Moreover, based on this PCA, organic matter content (LOI550) seems to negatively affect the ESTI, as sedimentation rate and organic matter content are negatively correlated ($p = 0.05$; $r = -0.7$). However, sedimentation rates and organic matter contents are related characteristics in these Alpine lakes as an increase in sedimentation rate causes a decrease in organic matter content (dominated by lacustrine organic matter) through dilution with detrital components. This negative correlation between organic matter content and ESTI also suggests that the gas production by organic matter decomposition does not affect significantly the sediment-slope stability of the studied lakes. Hence, a significant increase (decrease) of the sedimentation rate appears to be the dominant factor resulting in an increase (decrease) of the ESTI (Figure 5b). This suggests that the sedimentation rate strongly influences the lake sensitivity toward earthquake shaking. For long-term palaeoseismological

reconstructions, this implies that a significant change in sedimentation rates of a given lake can in turn induce a significant change in its sensitivity, a relationship already suggested in different lake systems [e.g., *Boe et al*., 2004; *Bertrand et al*., 2008; *Beck*, 2009; *Strasser et al*., 2013]. Hence, further studies aiming at improving the regional earthquake recurrence interval from the study of small lakes should control carefully that no significant change in sedimentation rates of up to 0.5 to 1 mm yr^{-1} occurs within the record. This aspect appears to be particularly crucial as changes in sedimentation rate change the threshold intensity required to form an identifiable deposit in a lake. Lower (higher) sedimentation rate causes an increase (decrease) in the recording threshold and a reduction (increase) of earthquake-triggered deposits in a lake, which for instance may be wrongly interpreted as evidence for clustering of earthquakes in time. However, if changes in sedimentation rate and recording threshold can be identified, accurate estimates of recurrence above the threshold can still be gained from intervals where the sedimentation rate is constant.

6. Conclusions

Eight sediment sequences from small alpine-type lakes of the western European Alps have been reviewed to reconstruct records of mass movement occurrences and to compare them to the well-documented historical seismicity. This comparison aimed at a better evaluation of the link between such deposits and their seismic trigger. Additionally, it aims at better linking mass movement occurrences to the corresponding epicentral locations and magnitudes of prehistoric earthquakes, both eventually improving the quality of paleoseismic reconstructions.

In the eight lake sequences, 34 MMDs have been identified and correspond to 24 mass movement occurrences. Their temporal correlations revealed that 12 of them are synchronous in neighboring lakes, which strongly supports an earthquake trigger mechanism. In addition, the comparison of the MMD ages to the historical earthquake dates increased this number to 21. These results suggest that a MMD identified in a small alpine-type lake is likely an indicator for an earthquake trigger. Hence, this type of lake appears to be a relevant target for paleoseismological reconstruction and recurrence-interval assessment. However, the number of MMDs varies between lakes in a same region, suggesting distinct sensitivities of the lake sequences to earthquake shaking, i.e., distinct slope stabilities. Diagrams of "epicentral intensity versus distance lake epicenter" allow lake sensitivity thresholds to be quantified. This sensitivity assessment, quantified with the ESTI parameter, opens new perspectives for paleoseismological reconstructions from lake sediments in moderately seismogenic areas with the possibilities to estimate (i) the location of past epicenters by choosing several lakes of equal sensitivity spread in a region of ~100 km and (ii) to estimate epicentral intensities of past regional earthquakes by choosing neighboring lakes of graded sensitivity. Finally, we compared the sensitivity thresholds to some lake and sedimentary parameters to better understand the origin of these variations in sensitivity. Our results suggest that the sedimentation rate appears to be the dominant factor explaining the lake sensitivity, i.e., that the lake sensitivity increases (decreases) when the sedimentation rate increases (decreases). This also means that the sensitivity of a single lake may substantially be altered by a decrease/increase in sedimentation rate.

Based on our results, further studies aiming at improve the paleoseismic event catalog based on small lakes should (i) focus on lake systems with sedimentation rates $\geq$0.5 mm yr^{-1} in moderately active seismotectonic regions, (ii) consider interlakes correlations over less than 100 km for epicentral earthquake intensity $<$IX, and (iii) control carefully that no significant change in sedimentation rates occurs within the record, which could make unstable the threshold condition and, thereby, falsify recurrence-interval assessment. However, to better constrain the link between lake sensitivity toward earthquake shaking and sedimentation rate, a wider lake compilation is still required (including also larger lakes), which may allow establishing more accurately recurrence intervals of past earthquakes.

Acknowledgments
Authors thank Estelle Ployon for her help in GIS assisting and Laurent Millet for constructive discussions. Radiocarbon dating of Lake DOS was performed by the national facility LMC14 in the framework of the INSU ARTEMIS call for proposal. We thank Jean-Pascal Dumoulin (LMC14), Sönke Szidat (LARA, University of Bern), and Tomasz Goslar (Poznan Radiocarbon Laboratory) for helps in the management of ^{14}C samples and results. Financial support that allowed the data acquisition of Lake DOS was provided by the French National Research Agency's Pygmalion project (ANR BLAN07-2_204489). Financial support that allowed the data acquisition of Lake FOR was provided by a grant from the AXA Research Fund (Wilhelm's postdoctoral fellowship). Data acquisition of Lake BRE was made possible thanks to the financial support of the Conseil Régional de Franche-Comté and the University of Franche-Comté (OREAS project). The data for this paper are available by contacting the corresponding author.

References

Ai, F., M. Strasser, B. Preu, T. J. J. Hanebuth, S. Krastel, and A. Kopf (2014), New constraints on the oceanographic vs. seismic control on submarine landslides initiation: A geotechnical approach off Uruguay and northern Argentina, *Geo Mar. Lett.*, *34*(5), 399–417.

Ambraseys, N. N. (1988), Engineering seismology, *Earthquake Eng. Struct. Dyn.*, *17*, 1–105.

Arnaud, F., V. Lignier, M. Revel, M. Desmet, M. Pourchet, C. Beck, F. Charlet, A. Trentesaux, and N. Tribovillard (2002), Flood and earthquake disturbance of 210Pb geochronology (Lake Anterne, North French Alps), *Terra Nova*, *14*, 225–232.

Arnaud, F., M. Revel-Rolland, D. Bosch, T. Winiarski, E. Chapron, M. Desmet, N. Tribovillard, and N. Givelet (2004), A reliable 300 years-long history of lead contamination in Northern French Alps from distant lake sediment records, *J. Environ. Monit.*, *6*(5), 448–456.

Arnaud, F., O. Magand, E. Chapron, S. Bertrand, X. Boës, F. Charlet, and M. A. Mélières (2006), Radionuclide dating (210Pb, 137Cs, 241Am) of recent lake sediments in a highly active geodynamic setting (Lakes Puyehue and Icalma—Chilean Lake District), *Sci. Total Environ.*, *366*, 837–850.

Avşar, U., A. Hubert-Ferrari, M. De Batist, G. Lepoint, S. Schmidt, and N. Fagel (2014), Seismically-triggered organic-rich layers in recent sediments from Göllüköy Lake (North Anatolian Fault, Turkey), *Quat. Sci. Rev.*, *103*, 67–80.

Bakun, W. H., and O. Scotti (2006), Regional intensity attenuation models for France and the estimation of magnitude and location of historical earthquakes, *Geophysic. J. Int.*, *164*, 596–610.

Baraza, J., and G. Ercilla (1994), Geotechnical properties of near-surface sediments from the Northwestern Alboran Sea slope [SW Mediterranean]: Influence of texture and sedimentary processes, *Mar. Georesour. Geotechnol.*, *12*, 181–200.

Beck, C. (2009), Late Quaternary lacustrine paleo-seismic archives in north-western Alps: Examples of earthquake-origin assessment of sedimentary disturbances, *Earth Sci. Rev.*, *96*(4), 327–344.

Becker, A., M. Ferry, and K. Monecke (2005), Multiarchive paleoseismic record of late Pleistocene and Holocene strong earthquakes in Switzerland, *Tectonophysics*, *400*, 153–177.

Ben-Menahem, A. (1976), Dating historical earthquakes by mud profiles of lake-bottom sediments, *Nature*, *262*, 200–202.

Bertrand, S., F. Charlet, E. Chapron, N. Fagel, and M. De Batist (2008), Reconstruction of the Holocene seismotectonic activity of the Southern Andes from seismites recorded in Lago Icalma, Chile, 39°S, *Palaeogeogr. Palaeoclimatol. Palaeoecol.*, *259*, 301–322.

Blaauw, M. (2010), Methods and code for 'classical' age-modelling of radiocarbon sequences, *Quat. Geochronol.*, *5*, 512–518.

Boe, R., O. Longwa, and A. Lepland (2004), Postglacial mass movements and their causes in fjords and lakes in western Norway, *Norw. J. Geol.*, *84*, 35–55.

Boës, X., S. B. Moran, J. King, M. N. Çağatay, and A. Hubert-Ferrari (2010), Records of large earthquakes in lake sediments along the North Anatolian Fault, Turkey, *J. Paleolimnol.*, *43*, 901–920.

Brisset, E., et al. (2012), A multidisciplinary investigation of a Holocene lake sediment sequence in the Southern French Alps at Lake Petit (Mercantour, 2200 m a,s,l,): History of a disturbed geosystem, *Quaternaire*, *23*(4), 309–319.

Brooks, G. R. (2015), An integrated stratigraphic approach to investigating evidence of paleoearthquakes in lake deposits of eastern Canada, *Geosci. Can.*, *42*(2), 247–261.

Cara, M., Y. Cansi, A. Schlupp, P. Arroucau, N. Béthoux, E. Beucler, and K. Van Der Woerd (2015), SI-Hex: A new catalogue of instrumental seismicity for metropolitan France, *Bull. Soc. Geol. Fr.*, *186*(1), 3–19.

Chapron, E., C. Beck, M. Pourchet, and J. F. Deconinck (1999), 1822 earthquake-triggered homogenite in Lake Le Bourget (NW Alps), *Terra Nova*, *11*, 86–92.

Chardon, D., and O. Bellier (2003), Geological boundary conditions of the 1909 Lambesc [Provence, France] earthquake: Structure and evolution of the Trévaresse ridge anticline, *Bull. Soc. Geol. Fr.*, *174*(5), 497–510.

Courboulex, F., et al. (2007), Seismic hazard on the French Riviera: Observations, interpretations and simulations, *Geophys. J. Int.*, *170*, 387–400.

Cushing, M., O. Bellier, S. Nechtschein, M. Sébrier, A. Lomax, P. Volant, P. Dervin, P. Guignard, and L. Bove (2008), A multidiscilinary study of a slow-slipping fault for seismic hazard assessment: The example of the Middle Durance Fault (SE France), *Geophys. J. Int.*, *172*(3), 1163–1178.

Darnault, R., Y. Rolland, D. Bourlès, R. Braucher, G. Sanchez, M. Revel, and S. Bouissou (2012), Timing of the last deglaciation revealed by receding glaciers at the Alpine-scale: Impact on mountain geomorphology, *Quat. Sci. Rev.*, *31*, 127–142.

Delacou, B., C. Sue, J. D. Champagnac, and M. Burkhard (2004), Present-day geodynamics in the bend of the western and central Alps as constrained by earthquake analysis, *Geophys. J. Int.*, *158*, 753–774.

Delaquaize, B. (1979), Etude géologique, hydrologique et limnologique dans une région de moyenne montagne: Le bassin versant des lacs de Laffrey et de Pétichet Unpublished Doctoral Dissertation, Univ. Scientifique et Médicale de Grenoble, 210 pp.

Dhouib, A., M. Zerhouni, and L. Glandut (2004), Variations of laboratory soils parameters and their relationships, in *International Symposia on the Identification and Determination of Soil and Rock Parameters for Geotechnical Design, on Shallow Foundations and on Ground Improvement*, vol. 2, edited by J.-P. Magnan, 655 pp., Presse des Ponts, Paris.

Doig, R. (1990), 2300 yr history of seismicity from silting events, in Lake Tadoussac, Charlevoix, Quebec, *Geology*, *18*(9), 820–823.

Doughty, M., N. Eyles, C. H. Eyles, K. Wallace, and J. L. Boyce (2014), Lake sediments as natural seismographs: Earthquake-related deformations (seismites) in central Canadian lakes, *Sediment. Geol.*, *313*, 45–67.

Eva, E., S. Pastore, and N. Deichmann (1998), Evidence for ongoing extensional deformation in the western Swiss Alps and thrust-faulting in the southwestern Alpine foreland, *J. Geodyn.*, *26*(1), 27–43.

Fäh, D., et al. (2011), ECOS-09 earthquake catalogue of Switzerland release 2011. Report and database Public catalogue, 17.4.2011. Swiss Seismological Service ETH Zürich, Report SED/RISK/R/001/20110417.

Fanetti, D., F. S. Anselmetti, E. Chapron, M. Sturm, and L. Vezzoli (2008), Megaturbidite deposits in the Holocene basin fill of Lake Como (southern Alps, Italy), *Palaeogeogr. Palaeoclimatol. Palaeoecol.*, *259*, 323–340.

Gani, M. R. (2004), From turbid to lucid: A straightforward approach to sediment gravity flows and their deposits, *Sediment. Rec.*, *2*, 4–8.

Garrett, E., L. Shennan, E. P. Watcham, and S. A. Woodroffe (2013), Reconstructing paleoseismic deformation, 1: Modern analogues from the 1960 and 2010 Chilean great earthquakes, *Quat. Sci. Rev.*, *75*, 11–21.

Girardclos, S., O. T. Schmidt, M. Sturm, D. Ariztegui, A. Pugin, and F. S. Anselmetti (2007), The 1996 AD delta collapse and large turbidite in Lake Brienz, *Mar. Geol.*, *24*, 137–154.

Goldberg, E. D. (1963), *Geochronology with 210Pb Radioactive Dating*, pp. 121–131, IAEA, Vienna.

Gregor, N., et al. (2014), Comparison of NGA-West2 GMPEs, *Earthquake Spectra*, *30*, 1179–1197.

Gürpinar, A. (2005), The importance of paleoseismology in seismic hazard studies for critical facilities, *Tectonophysics*, *408*, 23–28.

Howarth, J. D., S. J. Fitzsimons, R. J. Norris, and G. E. Jacobsen (2014), Lake sediments record high intensity shaking that provides insight into the location and rupture length of large earthquakes on the Alpine Fault, New Zealand, *Earth Planet. Sci. Lett.*, *403*, 340–351.

Kremer, K., G. Simpson, and S. Girardclos (2012), Giant Lake Geneva tsunami in AD 563, *Nat. Geosci.*, *5*(11), 756–757.

Lambert, J., and A. Levret-Albaret (1996), *Mille ans de Séismes en France. Catalogues d'Épicentres, Paramètres et Références*, Ouest-Editions ed., 78 pp., Presses Académiques, Nantes.

Larroque, C., B. Delouis, B. Godel, and J. M. Nocquet (2009), Active deformation at the southwestern Alps – Ligurian basin junction (France-Italy boundary): Evidence for recent change from compression to extension in the Argentera massif, *Tectonophysics*, *467*, 22–34.

Larroque, C., O. Scotti, and I. Ioualalen (2012), Reappraisal of the 1887 Ligurian earthquake [western Mediterranean] from macroseismicity, active tectonics and tsunami modelling, *Geophys. J. Int.*, *190*, 87–104.

Lee, H. J., S. K. Chough, K. S. Jeong, and S. J. Han (1987), Geotechnical properties of sediment cores from the southeastern Yellow Sea: Effects of depositional processes, *Mar. Geotechnol.*, *7*, 37–52.

Lignier, V. (2001), Les sédiments lacustres et l'enregistrements de la paléosismicité, étude comparative de différents cas dans le Quaternaire des Alpes Nord-Occidentales et du Tien-Shan Kyrghyze Thèse de doctorat, Univ. de Savoie.

Marçot, N., G. Verrhiest-Leblanc, S. Auclair, M. Fontaine, M. De Michele, D. Raucoules, L. Fissier, and J. L. Genois (2014), Séisme de l'Ubaye du 7 avril 2014—Rapport de retour d'expérience Rapport BRGM/RP-63789-FR / DREAL/D-0037-2014-SPR-URNM.

Meghraoui, M., B. Delouis, M. Ferry, D. Giardini, P. Huggenberger, I. Spottke, and M. I. Granet (2000), Active normal faulting in the Upper Rhine Graben and paleoseismic identification of the 1356 Basel earthquake, *Science*, *293*, 2070–2073.

Michetti, A. M., F. A. Audemard, and S. Marco (2005), Future trends in paleoseismology: Integrated study of the seismic landscape as a vital tool in seismic hazard analyses, *Tectonophysics*, *408*, 3–21.

Migowski, C., A. Agnon, R. Bookman, J. F. W. Negendank, and M. Stein (2004), Recurrence pattern of Holocene earthquakes along the Dead Sea transform revealed by varve-counting and radiocarbon dating of lacustrine sediments, *Earth Planet. Sci. Lett.*, *222*(1), 301–314.

Moernaut, J., M. De Batist, F. Charlet, K. Heirman, E. Chapron, M. Pino, R. Brümmer, and R. Urrutia (2007), Giant earthquakes in South-Central Chile revealed by Holocene mass-wasting events in Lake Puyehue, *Sediment. Geol.*, *195*, 239–256.

Moernaut, J., M. Van Daele, K. Heirman, K. Fontijn, M. Strasser, M. Pino, R. Urrutia, and M. De Batist (2014), Lacustrine turbidites as a tool for quantitative earthquake reconstruction: New evidence for a variable rupture mode in south central Chile, *J. Geophys. Res. Solid Earth*, *119*, 1607–1633, doi:10.1002/2013JB010738.

Monecke, K., F. S. Anselmetti, A. Becker, M. Sturm, and D. Giardini (2004), The record of historic earthquakes in lake sediments of Central Switzerland, *Tectonophysics*, *394*, 21–40.

Morgenstern, N. R. (1967), *Submarine Slumping and Initiation of Turbidity Currents*, edited by A. F. Richards, pp. 189–220, Mar. Geotechnique UP, Urbana, Ill.

Mugnier, J. L., A. Gajurel, P. Huyghe, R. Jayangondaperumal, F. Jouanne, and B. Upreti (2013), Structural interpretation of the great earthquakes of the last millennium in the central Himalaya, *Earth Sci. Rev.*, *127*, 30–47.

Mulder, T., and J. Alexander (2001), The physical character of subaqueous sedimentary density flows and their deposits, *Sedimentology*, *48*, 269–299.

Mulder, T., and E. Chapron (2011), Flood deposits in continental and marine environments: Character and significance, in *Sediment Transfer From Shelf to Deep Water—Revisiting the Delivery System RM*, *AAPG Stud. Geol.*, vol. 61, edited by S. C. Zavala, pp. 1–30.

Mulder, T., and P. Cochonat (1996), Classification of offshore mass movements, *J. Sediment. Res.*, *66*(1), 43–57.

Mulder, T., S. Migeon, B. Savoye, and J. C. Faugères (2001), Inversely graded turibidite sequences in the deep Mediterranean: A record of deposits from flood-generated turbidity currents?, *Geo Mar. Lett.*, *21*, 86–93.

Nomade, J., E. Chapron, M. Desmet, J. L. Reyss, F. Arnaud, and V. Lignier (2005), Reconstructing historical seismicity from lake sediments (Lake Laffrey, western Alps, France), *Terra Nova*, *17*, 350–357.

Passega, R. (1964), Grain-size representation by CM patterns as a geological tool, *J. Sediment. Petrol.*, *34*(4), 830–847.

Petersen, J., B. Wilhelm, M. Revel, Y. Rolland, C. Crouzet, F. Arnaud, E. Brisset, E. Chaumillon, and O. Magand (2014), Sediments of Lake Vens (SW European Alps, France) record large-magnitude earthquake events, *J. Paleolimnol.*, *51*(3), 343–355.

R Core Team (2012), R: A language and environment for statistical computing. [Available at http://www.r-project.org/.]

Reimer, P. J., M. G. L. Baillie, E. Bard, A. Bayliss, J. W. Beck, and P. G. Blackwell (2009), IntCal09 and Marine09 radiocarbon age calibration curves, 0–50,000 years cal BP, *Radiocarbon*, *51*, 1111–1150.

Renberg, I., R. Bindler, and M. L. Bränvall (2001), Using the historical atmospheric lead-deposition record as a chronological marker in sediment deposits in Europe, *Holocene*, *11*(5), 511–516.

Rodriguez-Pascua, M. A., V. H. Garduno-Monroy, I. Israde-Alcantara, and R. Pérez-Lopez (2010), Estimation of the paleoepicentral area from the spatial gradient of deformation in lacustrine seismites (Tierras Blancas Basin, Mexico), *Quat. Int.*, *219*, 66–78.

Sanchez, G., Y. Rolland, D. Schreiber, M. Corsini, J. M. Lardeaux, and G. Giannerini (2010), The active fault system of SW Alps, *J. Geodyn.*, *49*, 296–302.

Schnellmann, M., F. S. Anselmetti, D. Giardini, and J. A. McKenzie (2005), Mass-movement-induced fold-and-thrust belt structures in unconsolidated sediments in Lake Lucerne (Switzerland), *Sedimentology*, *52*, 271–289.

Schnellmann, M., F. S. Anselmetti, D. Giardini, and J. A. McKenzie (2006), 15,000 Years of mass movement history in Lake Lucerne: Implications for seismic and tsunami hazards, *Eclogae Geol. Helv.*, *99*, 409–428.

Scotti, O., D. Baumont, G. Quenet, and A. Levret (2004), The French macroseismic database SISFRANCE: Objectives, results and perspectives, *Ann. Geophys.*, *47*(2), 571–581.

Shiki, T., F. Kumon, Y. Inouchi, Y. Kontani, T. Sakamoto, M. Tateishi, H. Matsubara, and K. Fukuyama (2000), Sedimentary features of the seismo-turbidites, Lake Biwa, Japan, *Sediment. Geol.*, *135*, 37–50.

Stegmann, S., M. Strasser, F. S. Anselmetti, and A. Kopf (2007), Geotechnical in situ characterization of subaquatic slopes: The role of pore pressure transients versus frictional strength in landslide initiation, *Geophys. Res. Lett.*, *34*, L07607, doi:10.1029/2006GL029122.

Strasser, M., F. S. Anselmetti, F. Donat, D. Giardini, and M. Schnellmann (2006), Magnitudes and source areas of large prehistoric northern Alpine earthquakes revealed by slope failures in lakes, *Geology*, *12*, 1005–1008.

Strasser, M., S. Stegmann, F. Bussmann, F. S. Anselmetti, B. Rick, and A. Kopf (2007), Quantifying subaqueous slope stability during seismic shaking: Lake Lucerne as model for ocean margins, *Mar. Geol.*, *240*, 77–97.

Strasser, M., M. Hilbe, and F. S. Anselmetti (2011), Mapping basin-wide subaquatic slope failure susceptibility as a tool to assess regional seismic and tsunami hazards, *Mar. Geophys. Res.*, *32*, 331–347.

Strasser, M., K. Monecke, M. Schnellmann, and F. S. Anselmetti (2013), Lake sediments as natural seismographs: A compiled record of Late Quaternary earthquakes in Central Switzerland and its implication for Alpine deformation, *Sedimentology*, *60*, 319–341.

Sturm, M., and A. Matter (1978), Turbidites and varves in Lake Brienz (Switzerland): Deposition of clastic detritus by density currents, in *Modern and Ancient Lake Sediments*, edited by A. Matter and M. E. Tucker, *Int. Assoc. Sedimentol. Spec. Publ.*, *2*, 147–168.

Sue, C., F. Thouvenot, J. Fréchet, and P. Tricart (1999), Widespread extension in the core of the western Alps revealed by earthquake analysis, *J. Geophys. Res.*, *104*, 25,611–25,622.

Talling, P. J. (2014), On the triggers, resulting flow types and frequencies of subaqueous sediment density flows in different settings, *Mar. Geol.*, *352*, 155–182.

Thouvenot, F., et al. (1998), The Ml 5.3 Epagny (French Alps) earthquake of 1996 July 15: A long awaited event on the Vuache fault, *Geophys. J. Int.*, *135*, 876–892.

Thouvenot, F., J. Fréchet, L. Jenatton, and J. F. Gamond (2003), The Belledonne Border Fault: Identification of an active seismic strike-slip fault in the western Alps, *Geophys. J. Int.*, *155*, 174–192.

Tricart, P. (1984), From passive margin to continental collision: A tectonic scenario for the western Alps, *Am. J. Sci.*, *284*, 97–120.

Van Daele, M., W. Versteeg, M. Pino, R. Urrutia, and M. De Batist (2013), Widespread deformation of basin-plain sediments in Aysén fjord [Chile] due to impact by earthquake-triggered, onshore-generated mass movements, *Mar. Geol.*, *337*, 67–79.

Van Daele, M., et al. (2015), A comparison of the sedimentary records of the 1960 and 2010 great Chilean earthquakes in 17 lakes: Implications for quantitative lacustrine palaeoseismology, *Sedimentology*, *62*(5), 1466–1496.

Vasskog, K., A. Nesje, E. N. Støren, N. Waldmann, E. Chapron, and D. Ariztegui (2011), A Holocene record of snow avalanche and flood activity reconstructed from a lacustrine sedimentary sequence in Oldevatnet, western Norway, *Holocene*, *21*, 597–614.

Wiemer, G., J. Moernaut, N. Stark, P. Kempf, M. De Batptist, M. Pino, R. Urrutia, B. Ladrón de Guevara, M. Strasser, and A. Kopf (2015), The role of sediment composition and behavior under dynamic loading conditions on slope failure initiation: A study of a subaqueous landslide in earthquake-prone South-Central Chile, *Int. J. Earth Sci.*, *104*(5), 1439–1457.

Wilhelm, B., F. Arnaud, D. Enters, F. Allignol, A. Legaz, O. Magand, S. Revillon, C. Giguet-Covex, and E. Malet (2012), Does global warming favour the occurrence of extreme floods in European Alps? First evidences from a NW Alps proglacial lake sediment record, *Clim. Change*, *113*, 63–581.

Wilhelm, B., et al. (2013), Palaeoflood activity and climate change over the last 1400 years recorded by lake sediments in the north-west European Alps, *J. Quat. Sci.*, *28*(2), 189–199.

Wilhelm, B., P. Sabatier, and F. Arnaud (2015), Is a regional flood signal reproducible from lake sediments?, *Sedimentology*, *62*(4), 1103–1117.